# Correlated fluctuations in polymer networks

## A. R. Atilgan, T. Haliloglu, I. Bahar and B. Erman*

*Polymer Research Center and School of Engineering, Bogazici University, and Tubitak Advanced Polymeric Materials Research Center, Bebek 80815, Istanbul, Turkey*
(Received 8 October 1997; revised 27 December 1997)

Polymer micronetworks with Cayley tree and random topologies are compared. The fluctuations of junctions in random networks exhibit significant departures from the mean value corresponding to those in Cayley tree topology. Correlations among the fluctuations are examined for the two types of networks. Correlations are stronger, and cover longer distances along the chain contours in random networks, compared to those observed in Cayley trees. This is a consequence of the non-uniform spatial distribution of connected vertices in a random network, as opposed to Cayley trees in which chains extend between junctions located in successive tiers only. The relaxation spectra of the two types of networks are compared. The cumulative distribution of frequencies obeys a power law dependence on frequency, with exponents of 1.4 and 1.1 for trifunctional Cayley tree and random networks, respectively. These exponents are significantly smaller than the Debye value of 3 for regular three dimensional crystals. © 1998 Elsevier Science Ltd. All rights reserved.

(Keywords: correlated fluctuations; polymer networks)

## INTRODUCTION

The phantom network model of networks forms the basis of the theories of rubber elasticity[1]. Its foundations were established by James and Guth[2]. The importance of the model in interpreting molecular deformation, neutron scattering and effects of entanglements were realised much later, however[3-7].

The first systematic treatment of junction fluctuations for interpreting scattering from deformed phantom networks is given by Pearson[5] followed by different levels of generalisation by various authors[6,8,9]. A concise and complete derivation of junction fluctuations in phantom networks is given by Kloczkowski et al. for unimodal and bimodal networks having the topology of a Cayley tree[6]. This topology allows for a closed form solution of the problem. In a Cayley tree, depicted in *Figure 1a*, there is no randomness; there are no loops. Chains originating from junctions of the $i$th tier always terminate in junctions of the $(i+1)$st tier, and the junctions on the final tier are assumed to be fixed in space. In a real network, shown in *Figure 1b*, the operational definition of a tier becomes ambiguous. However, for establishing a framework of comparison with Cayley trees, it is possible to conceive virtual tiers, based on the spatial distribution of junctions in the neighborhood

of a central one. In such a network, the topology is random. A systematic treatment of fluctuations in random networks has not yet been attempted. In the present study, we evaluate the fluctuations in chain dimensions and in junction positions for a network with random topology, and show its differences from those of a network with Cayley tree topology.

## THEORY

### General formulation of the problem

The configurational factor for Gaussian networks is expressed as[4]

$$Z_N = K\exp(-\{\Delta R^T\}\Gamma\{\Delta R\}) \qquad (1)$$

Here $\{\Delta R\}$ is the $3N$ dimensional vector formed by the fluctuations $\{\Delta R_1, \Delta R_2,...,\Delta R_N\}$ of the junctions, the superscript $T$ denotes the transpose, $K$ is a constant, and $\Gamma$ is a symmetric matrix known as the Kirchhoff or valency–adjacency matrix in graph theory[10]. The elements of $\Gamma$ are given by

$$\Gamma_{ij} = \begin{cases} -\gamma & \text{if } i \neq j \\ -\Sigma_{i\neq j}\Gamma_{ij} & \text{if } i = j \end{cases} \qquad (2)$$

where $\gamma = 3/(2<r^2>_0$, $<r^2>_0$ being the unperturbed mean-square end-to-end distance of a single

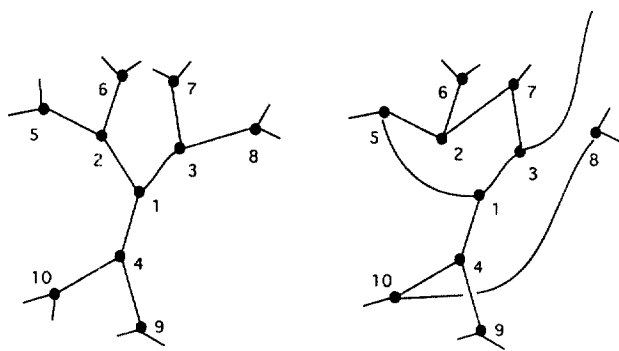*To whom correspondence should be addressed

**Figure 1** Schematic representation of phantom network models with (a) Cayley tree and (b) random topologies. Both models contain the same number of chains, all chains being of equal size, and both networks have functionality $\phi = 3$. They differ in that the Cayley tree contains no loops, and its junctions belong to successive tiers, starting from the innermost junction, labelled 1. In the random network, no hierarchy of junctions or polymer chains is distinguishable. Chains from different tiers (defined here in a virtual sense by analogy with a Cayley tree) may equally well be connected by a junction

network chain. The summation for evaluating $\Gamma_{ii}$ is performed over all off-diagonal elements on the $i$th column (or row). We note that $\Gamma$ is defined for two subsets of junctions, shortly referred to as fixed and fluctuating junctions, conveniently organised in submatrices[6]. In the following the submatrix associated with fluctuating junctions, only, is taken into consideration.

*Correlation between junction fluctuations*

The equilibrium correlation between the fluctuations of junctions $i$ and $j$ is given by[5,6]

$$< \Delta \mathbf{R}_i \cdot \Delta \mathbf{R}_j > = (3/2)(\Gamma^{-1})_{ij} \qquad (3)$$

In Cayley trees of infinite size, the average fluctuations of junctions $i$ and $j$ separated by $d$ other junctions along a path may be expressed by the matrix[6]

$$\begin{bmatrix} < (\Delta R_i^2) > & < \Delta \mathbf{R}_i \cdot \Delta \mathbf{R}_j > \\ < \Delta \mathbf{R}_i \cdot \Delta \mathbf{R}_j > & < (\Delta R_j^2) > \end{bmatrix} =$$

$$\frac{3}{2} \begin{bmatrix} (\Gamma^{-1})_{ii} & (\Gamma^{-1})_{ji} \\ (\Gamma^{-1})_{ij} & (\Gamma^{-1})_{jj} \end{bmatrix} = \frac{3}{2\gamma} \begin{bmatrix} \frac{\phi-1}{\phi(\phi-2)} & \frac{1}{\phi(\phi-2)(\phi-1)^d} \\ \frac{1}{\phi(\phi-2)(\phi-1)^d} & \frac{\phi-1}{\phi(\phi-2)} \end{bmatrix}$$

$$(4)$$

where $\phi$ is the junction functionality.

*Fluctuations in distances between junctions*

The mean-square fluctuations in the dimensions of the path $r_{ij}$ between junctions $i$ and $j$ are obtained[6] by substitution from equation (4) into

$$< (\Delta r_{ij})^2 > = < (\Delta \mathbf{R}_i - \Delta \mathbf{R}_j)^2 > = < (\Delta R_i)^2 >$$
$$+ < (\Delta R_j)^2 > -2 < \Delta \mathbf{R}_i \cdot \Delta \mathbf{R}_j > \qquad (5)$$
$$= 3/2[(\Gamma^{-1})_{ii} + (\Gamma^{-1})_{jj} - 2(\Gamma^{-1})_{ij}]$$

which leads to

$$\frac{< (\Delta r_{ij})^2 >}{<r^2>_0} = \frac{2}{\phi(\phi-2)} \frac{(\phi-1)^{d+1} - 1}{(\phi-1)^d} \qquad (6)$$

The Kirchhoff matrix for the Cayley tree shown in *Figure 1a* is given in previous work[6,8]. For the random network of *Figure 1b*, the matrix may be obtained by randomising the locations of the off-diagonal non-zero entries. For each junction of the micro-network, depending on the functionality, $\phi$ different random numbers are allocated by the random number generator which assigns equal weights to numbers in the interval [0,1]. The inverse of the matrix obtained in this manner cannot be expressed in closed form. In the present work, the inverse of $\Gamma$ and the analytical expressions given by equations (3)–(6) are evaluated numerically for trifunctional, tetrafunctional and 10-functional networks of 600, 300 and 900 chains, respectively, and the behaviours of the two types of networks with different topologies are compared.

## RESULTS AND DISCUSSION

*Junction fluctuations*

The mean-square fluctuations of junctions for tetrafunctional networks (i) in the form of a Cayley tree, and (ii) with a random topology are compared in *Figure 2*. The heavy and thin lines represent the results for the two respective cases. Networks comprising 302 junctions are considered here. Junctions are assigned numbers which increase with the number of tiers, as illustrated in *Figure 1*. The analytical solution given by equation (4) yields a constant ordinate value of 3/8 for the ratio $< (\Delta R_i)^2 > / <r^2>_0$ in a tetrafunctional infinite Cayley tree. In finite size Cayley trees, as the one presently considered, the fluctuation amplitudes decrease as the fixed junctions at the extremities of the tree are approached. The thick line in *Figure 2* displays this behaviour, the stepwise decreases referring to the passage from one tier to another. The thin line, however, displays the mean-square fluctuations of junctions in the tetrafunctional network of random topology. The fluctuations vary about the mean value of 3/8 of the infinite Cayley tree. However, significant scatter and dependence on junction location is observed in this case, similarly to the fluctuations of residues in protein
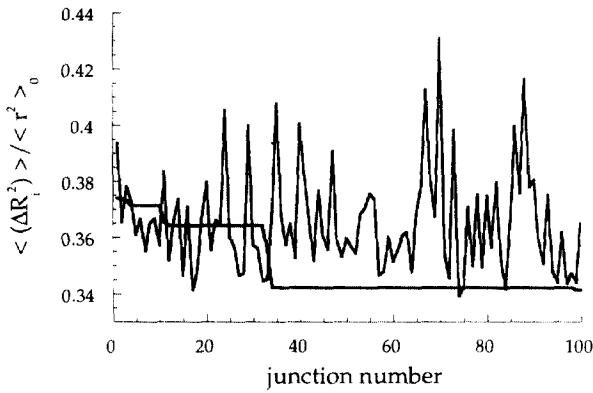
**Figure 2** Mean-square fluctuations in the junctions of tetrafunctional networks. The ordinate represents the fluctuations $< (\Delta R_i^2)>$ of the individual junctions $1 \leq i \leq N$ expressed relative to the unperturbed mean-square end-to-end separation $<r^2>_0$ of network chains. The thick line refers to a Cayley tree of 302 junctions while the thin line represents the behaviour of the junctions in a network of random topology. The mean value of the fluctuations for the random topology coincides with that (3/8) of the Cayley tree in the limit of infinite size networks. The stepwise decreases in the junction fluctuations for Cayley tree are associated with the passage from one tier to another, towards the fixed junctions on the exterior

crystals[11]. The similarity between the fluctuation behaviour of the two systems results from the similar form of their Kirchhoff matrices, which includes the effects of both chain connectivity and long-range (along the chain contour) associations. It is to be noted that the calculations are performed here for a single random network, representative of a quenched system.

## Fluctuations in chain dimensions

The mean-square fluctuation $<(\Delta r_{ij})^2>$ in the end-to-end separation of two junctions $i$ and $j$ separated by $d$ junctions is given by equation (6) for an infinite size Cayley tree. This relationship is
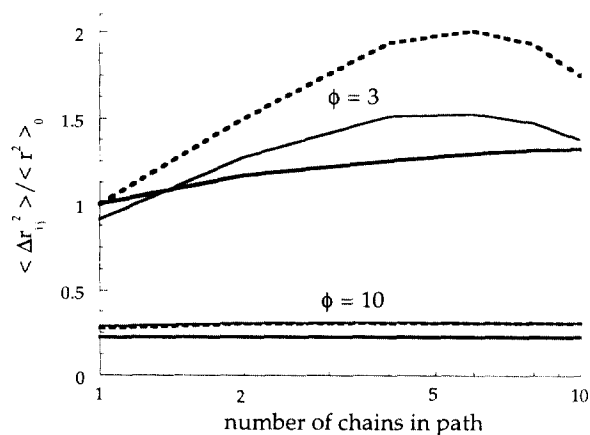


**Figure 3** Mean-square fluctuations in the distance $r_{ij}$ between junctions $i$ and $j$ separated by several junctions along a given path, plotted against the separation, in terms of the number of intervening junctions, between $i$ and $j$. Results are shown for trifunctional (upper curves) and 10-functional (lower curves) networks. Thick solid lines refer to infinite size Cayley trees [equation (6)]. Thin solid lines are their counterparts obtained numerically for finite size Cayley trees. The dashed lines represent the results for random topologies

illustrated in *Figure 3* (thick solid curves) for Cayley trees with functionalities $\phi = 3$ and 10. The fluctuations increase with the number of junctions in the path between junctions $i$ and $j$. For a trifunctional Cayley tree the fluctuations converge to a fixed value of 4/3 beyond approximately $d = 7$ chains along the path. In the case of tetrafunctional Cayley trees (not shown) the fluctuations converge to a fixed value at much shorter separations along the chain contour ($\approx 3$ intervening chains), while for 10-functional Cayley trees, practically no dependence on path length is observed. Alternatively, one can say that three and tetrafunctional Cayley trees are self-similar above length scales covering 7 and 3 chains, respectively, along a path. A 10-functional network with Cayley tree topology is self similar at all length scales.

The thin curves in *Figure 3* refer to the results from numerical calculations performed for finite size Cayley trees of $\phi = 3$ and 10. The difference between the thick and thin solid curves therefore reflects the finite size effects. In order to keep track of the junction identities $i$ and $j$ connected by a given number ($d$) of chains along the path, the following theorem is utilised:[12] junctions $i$ and $j$ are separated by ($d-1$) junctions if the $ij$th element of the matrix $\mathbf{A}^d$ is equal to one. Here $\mathbf{A}$ is the adjacency form of the Kirchhoff matrix $\Gamma$, the diagonal terms of which are equal to zero, and the non-zero off-diagonal elements are taken as one. The superscript $d$ denotes the $d$th power.

In *Figure 3*, the correlations for random networks are represented by dashed curves. For 10-functional networks, the curves for Cayley tree and random network topologies are almost indistinguishable. For trifunctional networks, however, random topology leads to stronger and longer-range correlations compared to those observed in Cayley trees. In a Cayley tree, each chain emanates from a junction that belongs to a well-defined branch, and inter-branch interactions are not permitted. In contrast, in the case of a random topology, inter-branch interactions are allowed through close circuits. These circuits, in turn, furnish the structure with additional spatial memory. The difference between the two topologies vanishes as the functionality increases because of extensive coverage of the three-dimensional space and the resulting effective decrease in the spatial separation between chains originally distant along a given path.

## Frequency distributions

The time evolution of cross-correlations between fluctuations of junctions $i$ and $j$ is conveniently expressed as a sum of exponentials[13]

$$< \Delta \mathbf{R}_i(0) \cdot \Delta \mathbf{R}_j(t) > = \sum_k A_{ij}^{(k)} \exp\{-\lambda_k t/\tau_0\} \quad (7)$$

Here $\lambda_k$ is the $k$th eigenvalue of $\Gamma$, $A_{ij}^{(k)}$ is the $ij$th element of the matrix $\lambda_k^{-1}\mathbf{u}_k\mathbf{u}_k^T$ formed by the $k$th eigenvalue and eigenvector $\mathbf{u}_k$ of $\Gamma$, and $\tau_0$ is a characteristic relaxation time. Thus, the time decay of correlations is determined by the eigenvalue distribution $g(\lambda)$, the eigenvalues $\lambda_k$ ($1 \le k \le N$) being representative of the frequencies of the $N$ modes of relaxation associated with the vibrational dynamics of the $N$ junctions. The eigenvalue spectrum is one of the fundamental characteristics of polymer networks[14,15].

In *Figure 4a*, the relaxation spectra $g(\lambda)$ are plotted for trifunctional (solid) and 10-functional (dashed) Cayley tree (thick lines) and random
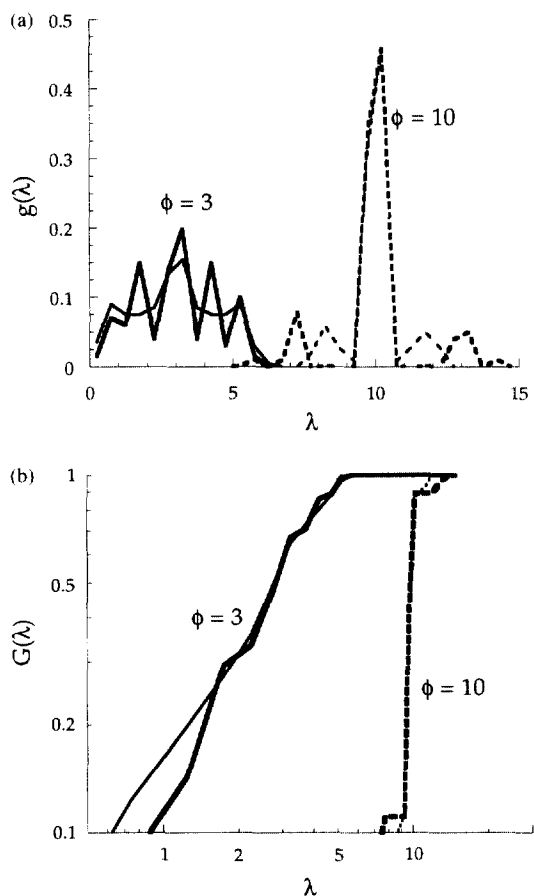


Figure 4 (a) Relaxation spectra for trifunctional and 10-functional networks. Solid lines refer to trifunctional networks, and among them the thinner ones represent the random topology. The dashed lines describe the 10-functional networks. The small peaks of the Cayley tree curve for $\phi = 10$ (thick dashed) are replaced in random networks by relatively more pronounced peaks closer to the central peak. (b) The cumulative distributions $G(\lambda)$ of frequencies, shown on a log–log scale. Thin solid line on the left refers to random trifunctional network. A power law of the form $G(\lambda) \sim \lambda^{1.1}$ is found for the trifunctional random network. The thick line, for trifunctional Cayley tree, yields an exponent of 1.4. Results for the 10-functional networks are displayed by the dashed lines. Both topologies exhibit a sharp increase at the frequency value equal to functionality. The thin dashed lines indicate the occurrence of a relatively smoother increase preceding and succeeding the abrupt jump in the case of random topologies

networks (thin lines). The peaks of the spectrum for the Cayley topology are derivable from the closed form expressions given before. The spectra for the trifunctional random networks are similar to those of the Cayley trees, except for the smoother distribution of frequencies in the former case, as expected from the irregularity of the chain connectivities in the random network topology. For the random 10-functional networks, the smaller peaks which are next to the central one in Cayley topology come closer to the main peak, whereas those which are further away from the central peak disappear.

The cumulative distributions $G(\lambda)$ of modes for the same networks are shown in *Figure 4b* in log–log form. Thick and thin curves refer to the Cayley tree and random topologies. Results of calculations for a three and ten functional network are shown. The initial slopes of the curves for the trifunctional Cayley tree and random topologies are $\beta = 1.4$ and 1.1, respectively, indicating a power law of the form $G(\lambda) \approx \lambda^\beta$ throughout a broad range of the spectrum. For a three dimensional regular crystal structure, the exponent $\beta$ is around 3, while for native proteins it varies in the range $1.5 \le \beta \le 2.0$[13,16]. The latter are characterized by an average functionality of seven. As the functionality of the networks increases, a stronger dependence on frequency (higher $\beta$) is observed. For the 10-functional networks, for example, a very sharp, anomalous increase is observed in the distributions both for Cayley tree and random topologies. The smaller peaks of *Figure 4a* contribute to the initial and the final stages of the cumulative distribution in *Figure 4b*.

## CONCLUSION

These results indicate that the polymer micronetwork structures exhibit unique vibrational characteristics strongly dependent on: (i) local packing density, expressed here by the junction functionalities; and (ii) topology, represented by the distribution or types of junctions: the Cayley tree represents one extreme topology in which only chains close along a given path are associated via junctions. In the random network topology, however, chains far apart along a given path may equally be connected at a given junction, and these long-range associations may have a drastic effect on the overall vibrational dynamics, as illustrated in *Figure 2*. Eigenvalues at the lower end of the spectrum for random micronetworks are smaller than those for the Cayley tree. Knowing that the free energy is linearly proportional to the smallest eigenvalue[14] the modulus of elasticity for random

networks will be lower than that for the Cayley networks. The question of whether these results obtained for micronetworks can be scaled to those for macronetworks would be very challenging.

The introduction of the topology of structure into the analysis, as carried out in the present work, may have far reaching applications in the field of condensed matter exhibiting large-scale fluctuations. Proteins in the native state form a good example. A macromolecular protein generally consists of 100–1000 amino acid side groups, or residues. In the native state, the residues are packed in an irregular crystalline order. The residues exhibit large amplitude fluctuations about their equilibrium configurations in the native state. The analogy to the Gaussian network is obvious. Each residue may be likened to a junction. The coordination number of each residue is analogous to the junction functionality of the network. The topology of the network is analogous to tertiary contacts in folded protein structures. Considering the analogies stated earlier, the statistical mechanics and dynamics of Gaussian networks have recently been applied to the analysis of thermal fluctuations of various native proteins[11,13].

## REFERENCES

1. Erman, B. and Mark, J. E., *Structures and Properties of Rubber-like Networks*. Oxford University Press, Oxford, 1997.
2. James, H. M. and Guth, E. J., *Chem. Phys.*, 1953, **21**, 1039.
3. Deam, R. T. and Edwards, S. F., *Phil. Trans. Roy. Soc. London*, 1976, **280**, 317.
4. Flory, P. J., *Proc. R. Soc. London, A*, 1976, **351**, 351.
5. Pearson, D. S., *Macromolecules*, 1977, **10**, 696.
6. Kloczkowski, A., Mark, J. E. and Erman, B., *Macromolecules*, 1989, **22**, 1423.
7. Kloczkowski, A., Mark, J. E. and Erman, B., *Macromolecules*, 1992, **25**, 2455.
8. Graessley, W. W., *Macromolecules*, 1980, **13**, 372.
9. Eichinger, B., *Ann. Rev. Phys. Chem.*, 1983, **34**, 359.
10. Eichinger, B., *Macromolecules*, 1972, **5**, 496.
11. Bahar, I., Atilgan, A. R. and Erman, B., *Folding and Design*, 1997, **2**, 173.
12. Cvetkovic, D., Rowlinson, P. and Simic, S., *Eigenspaces of Graphs*. Cambridge University Press, Cambridge, 1997.
13. Haliloglu, T., Bahar, I. and Erman, B., *Phys. Rev. Lett.*, 1997, **79**, 3090–3093.
14. Shy, L. Y. and Eichinger, B. E., *J. Chem. Phys.*, 1989, **90**, 5179.
15. Kloczkowski, A., Mark, J. E. and Frisch, H., *Macromolecules*, 1990, **23**, 3481.
16. Ben-Avraham, D., *Physical Review B*, 1993, **47**, 14559.